EGU-2011
2314-A96

A probabilistic approach to the discrimination of underwater acoustic signals generated by teleseismic P-waves

Alexey Sukhovich[1], Jean-Olivier Irisson[2], Anthony Ogé[1], Frederik J. Simons[3], Anne Deschamps[1], Yann Hello[1], and Guust Nolet[1]

(1) Géoazur, Sophia-Antipolis, France
(2) Observatoire Océanologique, Villefranche-sur-Mer, France
(3) Dept. Geosciences, Princeton University, Princeton NJ, USA

MOTIVATION

PROBLEM
A lack of data from *oceanic* regions:

• especially severe for southern hemisphere (Figure 1)

• southern hemisphere contains most of the known plumes

• imaging of plumes is important for better understanding of the dynamics of the mantle

GOAL
reduce the gap between the seismic data collected over land and oceanic regions for global seismic tomography → record arrivals of *teleseismic* P-waves.

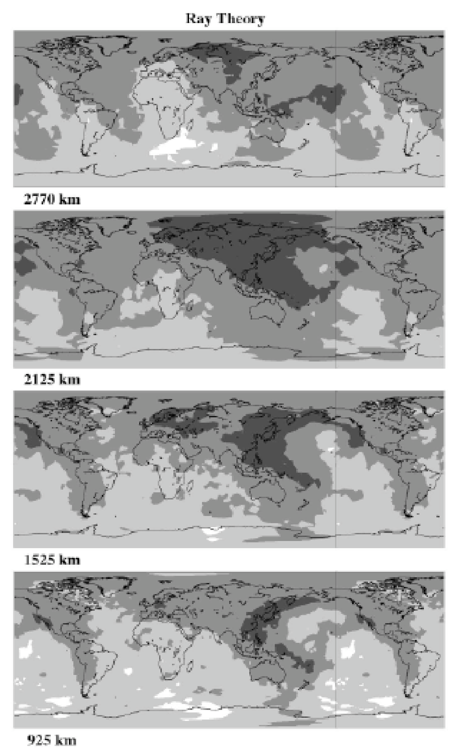

Figure 1 Ray density calculated by Montelli *et al.* (2004) for a global tomography study. Lighter areas indicate lower density of rays.

MERMAID - Mobile Earthquake Recording in Marine Areas by Independent Divers

IDEA
Seismic waves are converted into acoustic waves upon refraction at the crust/water interface → record acoustic signals generated by teleseismic P-waves.

MERMAID - RAFOS float (constructed by Teledyne Web Research) equipped with a hydrophone to detect acoustic signals generated by teleseismic P-waves (Figure 2; Simons *et al.*, 2009). The floats are freely drifting underwater robots with variable buoyancy → can dive to and remain at a given depth.

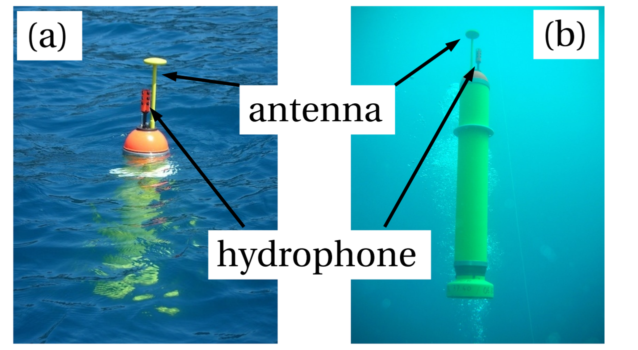

Figure 2 MERMAID prototype (a) at the surface and (b) in the process of surfacing. Indicated are an antenna for satellite communication and a hydrophone for recording of acoustic signals.

TYPICAL MISSION (Figure 3):

• Descent to a programmed depth (~1500 m)

• Continuous pressure monitoring

• On-board analysis of the detected signals → Ascent in case of a high certainty detection of a teleseismic P-wave

• Data transmission via satellite

• The cycle is repeated ...

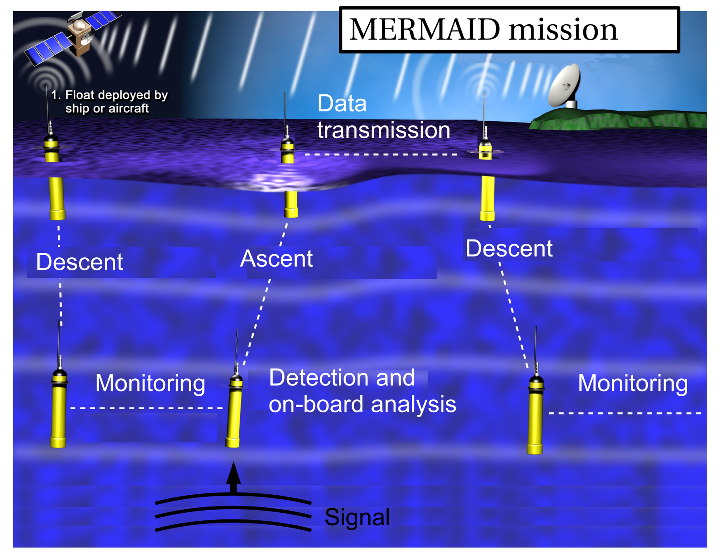

Figure 3 Mermaid mission. Not shown are *programmed* ascents (every 10 days) for the transmission of the signals which are less certain to be generated by teleseismic P-waves. These signals are stored in the robot's memory, but do not cause an immediate ascent (adopted from www.argo.ucsd.edu).

SIGNAL ANALYSIS

Oceans are full of signals generated by the sources other than teleseismic P-waves (ships, air guns, T-waves, whales, etc.) →
MERMAID must be able to *automatically* discriminate between signals of interest and those considered as noise.

To analyze the detected signals we are using **WAVELET TRANSFORM** – projection of a signal *f(t)* on a space defined by wavelet functions $\psi(t)$

Wavelet transform coefficient :

$$\gamma(s_j, \tau_i) = \int f(t)\, \psi^*\!\left(\frac{t-\tau_i}{s_j}\right) dt$$

where

τ_i - **translation factor** ⟺ **time**

s_j - **scale** ⟺ **frequency**

We perform wavelet transform with CDF(2,4) bi-orthogonal wavelets $\psi(t)$

The wavelet transform is visualized by means of a **SCALOGRAM** - absolute values of all wavelet transform coefficients $\gamma(s, \tau)$ as a function of s and τ (Figure 4).

Absolute value of a wavelet transform coefficient $\gamma(s_j, \tau_i)$ is proportional to the signal **power** in a given frequency band and at a given moment of time →

SCALOGRAM ⟺ **POWER DISTRIBUTION** in time and frequency domains

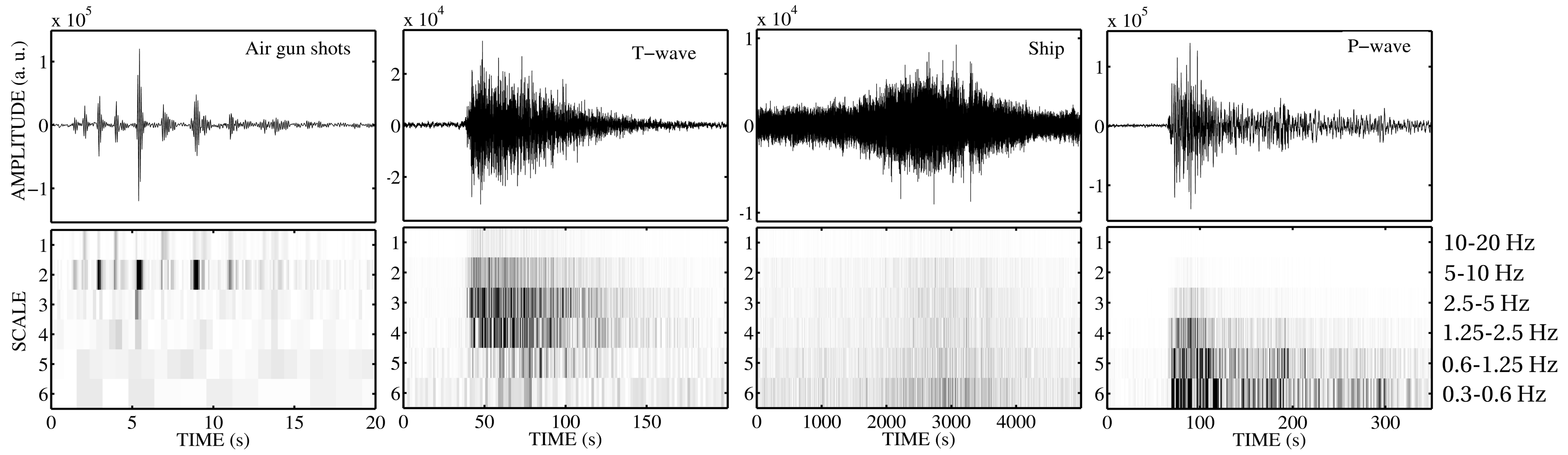

Figure 4 Sample scalograms of the signals detected by ocean bottom hydrophones (OBH). Note the identical time scale for the signal and its wavelet transform. Each scale corresponds to a certain frequency band – the lower scale correspond to higher frequencies. Each pixel in a scalogram represents a wavelet transform coefficients at a given time and in a given scale (frequency band). Coefficients with higher absolute values are indicated by darker colors.

SIGNAL RECOGNITION : STATISTICAL APPROACH

Once a signal is detected by a simple STA/LTA trigger:

• Estimate its *relative* **power distribution** among different scales (or frequency ranges).

• Normalize signal's power by the power of a *preceding* ambient noise record to remove influence of the noise variability.

• Compare normalized power distribution with a **STATISTICAL MODEL** for signals of known origin (P-waves in our case).

• Find the **probability** P that the detected signal is a P-wave (belongs to a P-wave statistical model) → decision whether MERMAID ascends or remains at a depth.

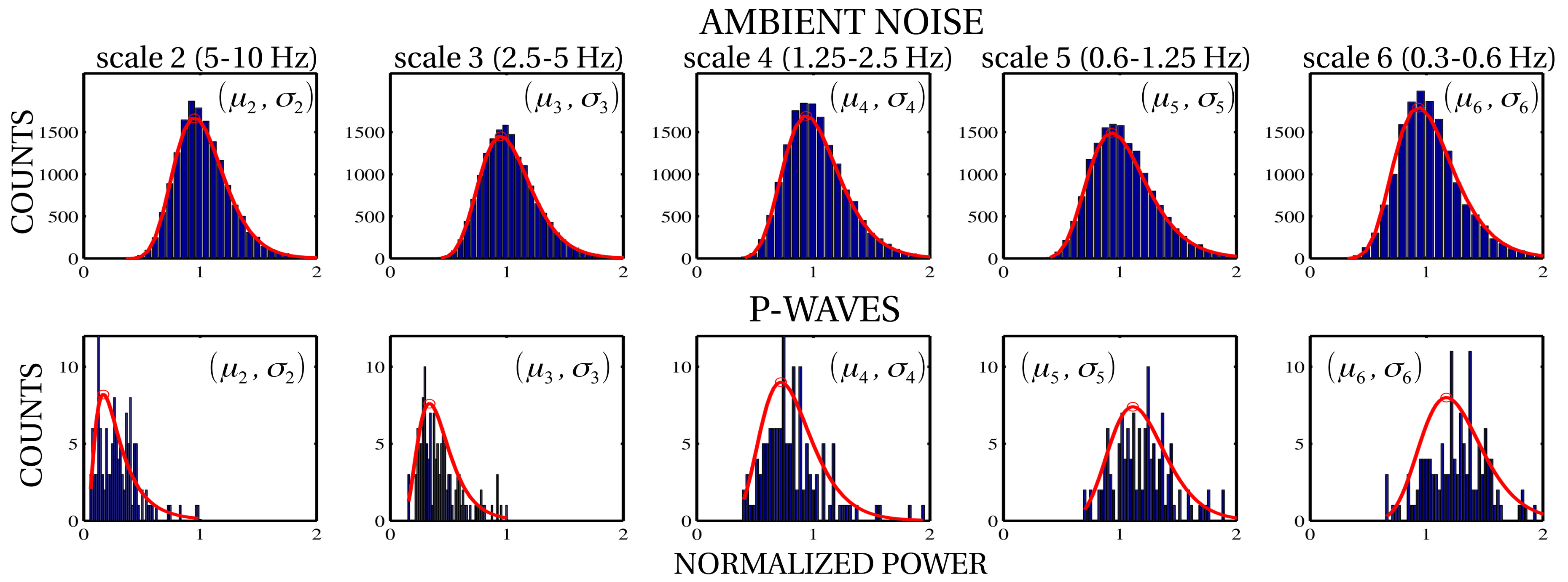

Figure 5 Histograms of the analyzed ambient noise records (top) and P-wave signals (bottom) used to deduce the statistical properties of the normalized power distributions. The values seem to follow the log-normal distribution law. For each scale we determine the mean and standard deviation of the distributions of the scale averages.
The set of values $(\mu_1, \sigma_1), \ldots, (\mu_K, \sigma_K)$ constitute a statistical model of a given type of the signal.

STATISTICAL MODEL

The statistical model for the signals of a certain type is obtained from statistical properties (mean and standard deviation) of the normalized power distributions of a large number of signals of the *same* origin →

$$(\mu_1, \sigma_1), \ldots, (\mu_K, \sigma_K)$$

where K is a number of scales

To obtain statistical models, we analyzed the data acquired during the Grosmarin experiment – 7 OBHs deployed in the Ligurian Sea at the depth 1300 – 2400 m and *continuously* recording during 6 months (Dessa *et al.*, 2011).

Figure 5 shows the histograms of the normalized power distributions for the ambient noise records and signals generated by teleseismic P-waves (a total of 128 signals of P-waves were used to create the P-waves model). These histograms were used to determine μ and σ for each scale.

Figure 6 compares all the statistical models obtained from the Grosmarin data. Note the significant differences between the statistical model of P-waves and those of the signals of other origin (ships, air guns, T-waves) → Recognition is possible!

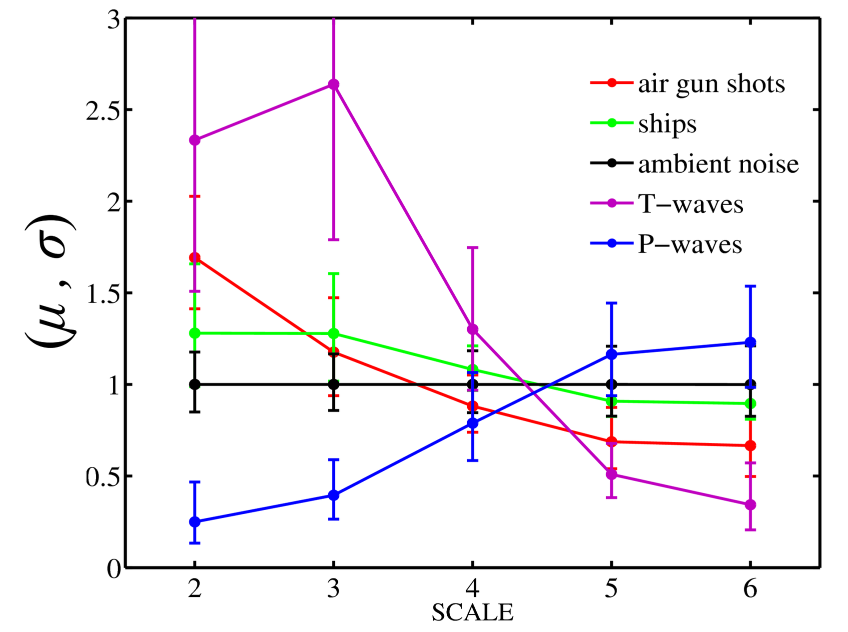

Figure 6 Statistical models for the signals of different origins. Note the substantial difference between the model for the P-wave signals and other models. Vertical bars denote one standard deviation.

RESULTS

Our approach was tested on the data of the Grosmarin experiment by applying the recognition scheme to each 2-hour-long record.

For each detected signal the probability P was calculated for the signal to be a P-wave. The signal was recognized as a P-wave when $P > P_0$ and rejected when $P < P_0$, where P_0 was a predefined probability threshold.

Figure 7 shows the recognition results as a function of the threshold P_0 and SNR of the detected signals for two the most important cases for us :
- P-wave signals recognized as P-waves
- Signals of other origin recognized as P-waves ("false positives")

For the success of the mission it is of utmost importance to *eliminate* or reduce the number of false positives because each surface/depth cycle depletes the battery and reduces the robot's lifetime.

Figure 7 allows to *visualize* the choice of the P_0 and minimum SNR of the detected signals : by choosing P_0=0.2 and retaining only signals with SNR > 2.5, *no* false positive recognitions are expected. With this set of parameters, we detect 87% of all the P-wave signals.

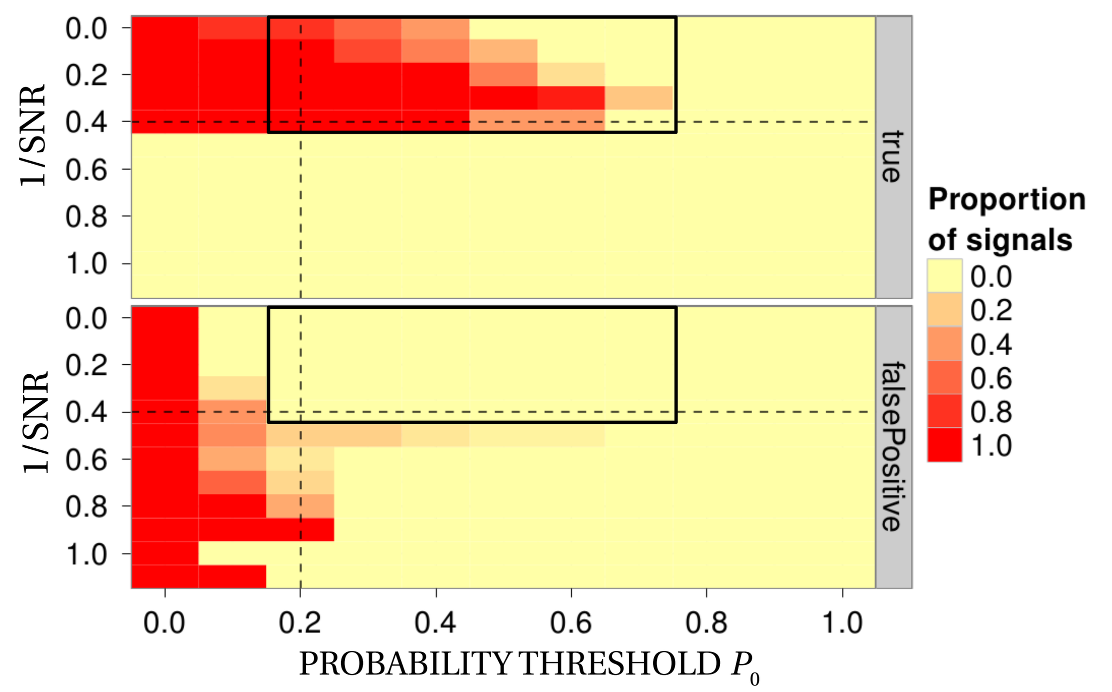

Figure 7 Number of correct (top) and false positive (bottom) recognitions as function of the threshold P_0 and SNR. The number of signals in each SNR group is normalized by the maximum number of signals in the same group and thus varies from 1 (P_0 = 0) to 0 (P_0 = 1). The region of no false positive recognitions is indicated by the black solid line.

CONCLUSIONS

• *Automatic* recognition scheme based on the statistical analysis of the distribution of the power of the detected signal among different frequency bands is designed.

• P-waves *can* be recognized unambiguously if SNR > 2.5 !

• By properly choosing probability and SNR thresholds, false recognitions can be eliminated.

REFERENCES
Dessa *et al.*, *Bulletin de la Société géologique de France*, in press (2011)
Montelli *et al.*, *Geophysical Journal International* **158**, 637-654 (2004)
Simons *et al.*, *Journal of Geophysical Research* **114**, B05307 (2009)